MINERALOGICAL MAGAZINE, MARCH 1973, VOL. 39, PP. 36–48

The crystal chemistry of the amphiboles. I: Refinement of the crystal structure of ferrotschermakite

F. C. HAWTHORNE AND H. D. GRUNDY

Dept. of Geology, McMaster University, Hamilton, Ontario, Canada

SUMMARY. Three-dimensional counter-diffractometer data and a full-matrix least-squares method have been used to refine the crystal structure of a ferrotschermakite in the space group $C2/m$. The chemical composition of the amphibole is $Na_{0\cdot23}K_{0\cdot14}Ca_{1\cdot86}Mg_{1\cdot22}Fe^{2+}_{2\cdot10}Mn_{0\cdot02}Ti_{0\cdot10}Fe^{3+}_{0\cdot30}Al_{1\cdot30}Al_{2\cdot00}Si_{6\cdot00}O_{22}(OH)_2$ with cell parameters a 9·8179(7), b 18·1060(14), c 5·3314(5) Å, and β 105·00(1). Cation site-occupancies were initially assigned by ionic-radius criteria and refined with the constraint that the sum total of the site-occupancies be equal to the chemical analysis.

The A-site shows positional and substitutional disorder and can be better represented by two sites, one on the mirror plane and the other on the 2-fold axis.

Unit weights were used throughout the refinement and the final R-factor for 1207 observed non-equivalent reflections was 4·5 %.

ALTHOUGH there has been much work on the crystallography of the amphiboles in recent years, many details of their crystal chemistry remain obscure due to the chemical complexity of these minerals. The presence of many similar but non-equivalent sites leads to complicated cation site-occupancies, which have been considered by some authors to reflect temperatures of equilibration of mineral assemblages. Before any quantitative use can be made of the amphiboles in this respect, it is necessary to know the effect of bulk composition on this site disorder. Because of the wide range in chemistry of these minerals, much structural information is needed concerning the various possible cationic substitutions. With this in mind, a structural refinement of a ferrotschermakite was made in order to examine the site-partitioning and details of the A-site configuration in a highly aluminous amphibole.

Unit cell and space group. The amphibole used in this investigation was from Frood Mine, Sudbury, and was supplied by the International Nickel Co. of Canada. Optically, the crystals show no signs of zoning or exsolution. The amphibole was separated by a combination of magnetic susceptibility and heavy liquid techniques, and finally hand-picked; the final estimate of the purity of the sample was > 99 %. The material was analysed by conventional wet chemical techniques and the analysis is given in table I.

Single-crystal precession photographs display diffraction symmetry $2/mC-/-$ consistent with space groups $C2$, Cm, and $C2/m$. A statistical test made on the data indicated the presence of a centre of symmetry, and thus the space group $C2/m$ was

used in the refinement. The unit cell parameters were determined by a least-squares method from 31 intense reflections collected on a 4-circle single-crystal diffractometer; these are presented in table I.

Intensity data. A well-shaped crystal showing the {110} form was chosen in order to facilitate absorption corrections. The crystal was slightly elongate along the crystallographic *c* direction; the dimensions were 0·074×0·104×0·140 mm.

TABLE I. *Crystal data*

		Atomic ratios‡			
SiO_2	40·12†	Si	6·00		
TiO_2	0·87	Al^{iv}	2·00		
Al_2O_3	18·67	Tetrahedral Σ	8·00		
Fe_2O_3	2·64	Al^{vi}	1·30		
FeO	16·75	Fe^{3+}	0·30		
MnO	0·27	Fe^{2+}	2·10	Space Group	*C*2/*m*
MgO	5·48	Mg	1·22	*Z*	2
CaO	11·65	Mn	0·02	Linear absorption coefficient	32·5 cm^{-1}
Na_2O	0·80	Ti	0·10	Crystal size	0·074×0·104×0·140 mm
K_2O	0·75	Octahedral Σ	5·04	Radiation/filter	Mo/Zr
H_2O^+	1·61	Ca	1·86	Crystal axis for data collection	[10$\bar{1}$]*
H_2O^-	0·01	Na	0·23	No. of non-equivalent	1217
F	0·07	K	0·14	$\|F_0\| > 0$	
	99·69				
Less		Large cation Σ	2·23	Final *R* (unit weights)	0·045
O ≡ F	0·03			Average $\sigma\|F\|$	1·96
Total	99·66				

† Analysis by John Muysson, Dept. of Geology, McMaster University, Hamilton, Canada.
‡ Calculation based on 23 oxygens excluding H_2O.

The intensity data were collected on a GE–XRD6 automatic 4 circle diffractometer equipped with a 1/4 circle. Zr-filtered Mo radiation (λ = 0·71069 Å), a scintillation counter, and a pulse height analyser set to pass 90 % of the energy distribution were used during data collection. The θ–2θ scan method was employed with a scan rate of 2°/min. The scan range was computed using the formula 1·80+tan θ (Alexander and Smith, 1964) and a 20-second fixed-background count made at the beginning and end of the scan.

4887 reflections were gathered up to 65° 2θ over three asymmetric units. The data were corrected for absorption using an eight point gaussian-quadrature integration for polyhedral crystal shape (programme from Cornell University), for background, Lorenz, and polarization effects. Equivalent reflections were averaged to produce an asymmetric set. The resulting F_0 were classed as unobserved if their magnitude fell below that of three times the standard deviation based on counting statistics. This procedure resulted in 1767 unique reflections of which 560 were classed as unobserved.

Refinement of the structure.[1] The final coordinates and temperature factors of Kakanui hornblende (Papike *et al.*, 1969) were used as initial parameters for the least-squares programme. Atomic scattering factors for fully ionized atoms were taken from Doyle and Turner (1968), Tokonami (1965), and Cromer and Mann (1968).

One cycle of full-matrix least-squares refinement varying the atomic positions[2] reduced the *R*-factor from 45 % to 19 %, where $R = \Sigma |F_0 - F_{calc}| / \Sigma F_0$. The site occupancies were then adjusted to agree with the chemical formula and the *M*(1) and *M*(3) occupancies varied, during which the *R*-factor fell from 12 % to 9·4 %. On varying the isotropic temperature factors with everything else constant the *R*-factor dropped to 7·2 %. Numerous subsequent refinements of positions, temperature factors, and site occupancies resulted in an *R* of 6·0 %. Examination of difference Fourier maps at this stage revealed a peak about 1 electron/Å^3 high in the vicinity of the hydrogen atom located in tremolite by Papike *et al.* (1969); the position was inserted into the least-squares programme and refined, with no resulting change in the *R*-factor. On the basis of Fourier sections through the *A*-site (discussed later) and the regular distribution of peaks and troughs in difference Fourier sections, it was decided to consider the *A*-site as positionally disordered both in the mirror plane and along the 2-fold axis. Further cycles of refinement reduced the *R*-factor to 5·9 %.

The temperature factors were then converted to anisotropic and one cycle resulted in the *R*-factor dropping to 4·7 %. The parameters at this stage were input into a least-squares programme by L. W. Finger (Finger, 1969*a*, *b*) and a further refinement of the structure was made with the sum of the site chemistries constrained to equal the bulk chemistry of the crystal as determined by chemical analysis. Slight changes occurred in all the refined parameters and the structure converged at an *R*-factor of 4·5 %. The final positional parameters and equivalent isotropic temperature factors are presented in table II. Interatomic distances and angles were computed using the programme ERRORS (Finger, 1969 and personal communication) in which the associated standard deviations are those obtained from the full matrices of errors both in atomic positions and cell parameters. These are presented in tables III and IV respectively.

Topology of the structure. The general features of the clinoamphibole structure have been discussed in detail (Papike *et al.*, 1969) and will only be briefly considered here. Fig. 1 illustrates the basic clinoamphibole structure, where strips of octahedrally coordinated cations are linked by double chains of SiO_4 tetrahedra. There are two non-equivalent tetrahedral cation sites, both in general positions; these are repeated by the symmetry to give the infinite double chains parallel to the *c*-axis that are characteristic of the amphiboles. The chains are arranged in layers parallel to (100) and sandwiched between these layers are the remaining cation sites, all of which are on special positions.

[1] Where not stated, all computer programs used are from X-ray 67, Program System for X-ray Crystallography, by J. M. Stewart, University of Maryland, adapted by H. D. Grundy for the CDC 6400.

[2] Scaling of the observed data was accomplished through a scale factor that was included as a parameter in the refinement and allowed to vary at all times.

There are three octahedral sites $M(1)$, $M(2)$, and $M(3)$ which are linked to form infinite strips parallel to c. The juxtaposition of the octahedral strips and tetrahedral chains gives rise to the $M(4)$ site, which may be approximated by a cubic antiprism. The large A-site lies between the octahedral strips and protrudes into the tetrahedral layers on each side of it. It is surrounded by 12 tetrahedral bridging oxygens.

TABLE II. *Atom site and populations*

Site	x	y	z	B*	Population
$O(1)$	0·1046(4)	0·0936(2)	0·2099(7)	1·01(5)	1·00 O^{2-}
$O(2)$	0·1198(4)	0·1766(2)	0·7419(7)	0·80(5)	1·00 O^{2-}
$O(3)$	0·1136(6)	0	0·7126(10)	0·99(7)	1·00 O^{2-}
$O(4)$	0·3713(4)	0·2511(2)	0·7951(7)	0·89(5)	1·00 O^{2-}
$O(5)$	0·3516(4)	0·1401(2)	0·1093(7)	0·99(5)	1·00 O^{2-}
$O(6)$	0·3418(4)	0·1206(2)	0·6021(7)	1·01(5)	1·00 O^{2-}
$O(7)$	0·3323(6)	0	0·2861(12)	1·39(5)	1·00 O^{2-}
$T(1)$	0·2799(1)	0·0864(1)	0·3012(3)	0·59(2)	See Table V
$T(2)$	0·2926(1)	0·1736(1)	0·8161(2)	0·59(2)	See Table V
$M(1)$	0	0·0902(1)	1/2	0·65(2)	0·610(5) Fe^{2+} + 0·390(5) Mg^{2+}
$M(2)$	0	0·1782(1)	0	0·55(2)	0·15 Fe^{3+} + 0·05 Ti + 0·65 Al^{3+} + + 0·100(5) Mg^{2+} + 0·050(5) Fe^{2+}
$M(3)$	0	0	0	0·60(2)	0·780(7) Fe^{2+} + 0·220(7) Mg^{2+}
$M(4)$	0	0·2806(1)	1/2	0·85(2)	0·01 Mn^{2+} + 0·05 Na^{+} + + 0·93 Ca^{2+} + 0·010(6) Mg^{2+}
$A(2)$	0	0·4784(17)	0	1·30(5)	$(Na_x + K_y)$ $\left.\vphantom{\begin{matrix}a\\b\end{matrix}}\right\}$ $x + 1{\cdot}8y$
$A(m)$	0·0272(34)	1/2	0·0621(63)	1·74(7)	$(Na_{0\cdot13-x} + K_{0\cdot14-y})$ $\left.\vphantom{\begin{matrix}a\\b\end{matrix}}\right\}$ = 0·080(9)
H	0·202(14)	0	0·784(26)	1/2	0·99 H^{+}

* $B_{\text{equiv. isotropic}}$

Octahedral cation site chemistry. Assignment of cations to the various non-equivalent sites in this amphibole may be accomplished by a combination of X-ray and crystal-chemical techniques.

Bond-length calculations made early in the refinement showed that the mean metal–oxygen distance for $M(2)$ was significantly smaller than those for $M(1)$, $M(3)$, and $M(4)$. This was consistent with an essentially ordered octahedral aluminium content and thus all the available octahedral aluminium was assigned to $M(2)$; the deficiency remaining was filled with the available Ti and Fe^{3+} in accord with work on infrared spectra (Bancroft and Burns, 1969), which indicated that the majority of Fe^{3+} ions occupy $M(2)$ positions in alkali amphiboles; this conclusion is also borne out by size criteria since the effective crystal radius of octahedrally coordinated Fe^{3+} (high spin) is less than those of the other remaining octahedral cations (Shannon and Prewitt, 1969).

The mean metal-oxygen distance for $M(4)$ was significantly larger than those of $M(1)$ and $M(3)$, and consistent with previous work (Papike *et al.*, 1969; Robinson

TABLE III*a*. *Bond multiplicities and interatomic distances in ferrotschermakite*

T(1) *Tetrahedron*		
T(1)–*O*(1)	1	1·668(4) Å
T(1)–*O*(5)	1	1·692(4)
T(1)–*O*(6)	1	1·679(4)
T(1)–*O*(7)	1	1·656(2)
Mean *T*(1)–*O*		1·674
M(1) *Octahedron*		
M(1)–*O*(1)	2	2·067(5)
M(1)–*O*(2)	2	2·170(5)
M(1)–*O*(3)	2	2·131(4)
Mean *M*(1)–*O*		2·123
M(2) *Octahedron*		
M(2)–*O*(1)	2	2·014(4)
M(2)–*O*(2)	2	2·029(5)
M(2)–*O*(4)	2	1·928(5)
Mean *M*(2)–*O*		1·990
A(*m*) *Polyhedron*		
A(*m*)–*O*(5)	2	3·042(4)
A(*m*)–*O*(5)	2	3·114(4)
A(*m*)–*O*(6)	2	2·905(5)
A(*m*)–*O*(6)	2	3·433(6)
A(*m*)–*O*(7)	1	2·504(7)
A(*m*)–*O*(7)	1	2·584(7)
A(*m*)–*O*(7)	1	3·391(8)
A(*m*)–*O*(7)	1	4·084(10)
Mean for 12		3·129
Mean for 8		2·901
Conventional A Site		
A–*O*(5)	4	3·056(4)
A–*O*(6)	4	3·159(3)
A–*O*(7)	2	2·518(4)
A–*O*(7)	2	3·735(4)
Mean for 12		3·114
A–*T*		
A(*m*)–*T*(1)		3·228(13)
A(*m*)–*T*(2)		3·413(28)
A(2)–*T*(1)		3·402(4)
A(2)–*T*(2)		3·583(2)
T(1)–*T*(2)		
T(1)–*T*(2) [through *O*(6)]		3·140(2)
T(1)–*T*(2) [through *O*(5)]		3·060(2)
T(1)–*T*(1) [across mirror]		3·130(3)

T(2) *Tetrahedron*		
T(2)–*O*(2)	1	1·640(4) Å
T(2)–*O*(4)	1	1·620(4)
T(2)–*O*(5)	1	1·636(4)
T(2)–*O*(6)	1	1·656(4)
Mean *T*(2)–*O*		1·638
M(3) *Octahedron*		
M(3)–*O*(1)	4	2·141(4)
M(3)–*O*(3)	2	2·115(6)
Mean *M*(3)–*O*		2·132
M(4) *Polyhedron*		
M(4)–*O*(2)	2	2·410(4)
M(4)–*O*(4)	2	2·330(5)
M(4)–*O*(5)	2	2·636(6)
M(4)–*O*(6)	2	2·519(4)
Mean *M*(4)–*O*		2·474
A(2) *Polyhedron*		
A(2)–*O*(5)	2	2·739(27)
A(2)–*O*(5)	2	3·388(30)
A(2)–*O*(6)	2	2·901(22)
A(2)–*O*(6)	2	3·441(27)
A(2)–*O*(7)	2	2·548(9)
A(2)–*O*(7)	2	3·756(9)
Mean for 12		3·129
Mean for 8		2·894
M–*M*		
M(1)–*M*(1)		3·266(2)
M(1)–*M*(2)		3·106(1)
M(1)–*M*(3)		3·126(1)
M(1)–*M*(4)		3·448(2)
M(2)–*M*(3)		3·226(2)
M(2)–*M*(4)		3·247(1)
Miscellaneous		
A(*m*)–*A*(*m*′)		0·735(2)
A(2)–*A*(2′)		0·784(7)
A(*m*)–*A*(2)		0·537(7)
O(3)–*H*		0·85(12)

et al., 1969) all Ca^{2+} was assigned to this site. Mn^{2+} and excess Fe^{2+} was assigned to $M(4)$ (see Papike *et al.*, 1969, p. 124) and the rest of the site was filled with Na^{+}. Excess Na^{+} and K^{+} was assigned to A. The site occupancies resulting from refinement with bulk chemical constraints on Mg^{2+} and Fe^{2+} are given in table II.

TABLE III*b*. *Oxygen–oxygen polyhedral edge lengths*

T(1) Tetrahedron		*T(2) Tetrahedron*	
O(1)–*O*(5)	2·748(5) Å	*O*(2)–*O*(4)	2·763(5) Å
O(1)–*O*(6)	2·741(9)	*O*(2)–*O*(5)	2·673(8)
O(1)–*O*(7)	2·750(6)	*O*(2)–*O*(6)	2·679(5)
O(5)–*O*(6)	2·677(5)	*O*(4)–*O*(5)	2·655(5)
O(5)–*O*(7)	2·730(4)	*O*(4)–*O*(6)	2·563(5)
O(6)–*O*(7)	2·745(5)	*O*(5)–*O*(6)	2·704(5)
Mean *O*–*O*	2·732	Mean *O*–*O*	2·673
M(1) Octahedron		*M(3) Octahedron*	
$O(1^u)$–$O(2^d)$*	2·733(5)	$O(1^u)$–$O(1^d)$	2·617(10)
$O(1^u)$–$O(2^u)$	3·178(5)	$O(1^u)$–$O(1^u)$	3·390(7)
$O(1^u)$–$O(3^d)$	2·844(5)	$O(1^u)$–$O(3^d)$	2·844(5)
$O(1^u)$–$O(3^u)$	3·153(6)	$O(1^u)$–$O(3^u)$	3·167(6)
O(2)–*O*(2)	3·007(11)	Mean *O*–*O*	3·004
O(2)–*O*(3)	3·201(3)	*M(4) Polyhedron*	
O(3)–*O*(3)	2·738(11)	*O*(2)–*O*(2)	3·007(11)
Mean *O*–*O*	2·998	$O(2^u)$–$O(4^u)$	3·170(5)
M(2) Octahedron		$O(2^u)$–$O(4^d)$	2·847(5)
O(1)–*O*(1)	2·617(10)	$O(2^u)$–$O(5^u)$	3·407(5)
$O(1^u)$–$O(2^d)$	2·733(5)	$O(4^u)$–$O(5^d)$	3·314(5)
$O(1^u)$–$O(2^u)$	2·949(5)	$O(4^u)$–$O(6^u)$	2·563(5)
O(1)–*O*(4)	2·822(5)	$O(5^u)$–$O(6^u)$	2·677(5)
$O(2^u)$–$O(4^d)$	2·847(5)	$O(5^u)$–$O(6^d)$	3·026(8)
$O(2^u)$–$O(4^u)$	2·776(5)	$O(6^u)$–$O(6^d)$	3·547(8)
O(4)–*O*(4)	2·822(11)	Mean *O*–*O*	3·035
Mean *O*–*O*	2·813		

* The superscript notation refers to oxygen x coordinate greater (u) or less (d) than the x coordinate of M.

Although detailed discussion of these results will be deferred to a later paper, some comment is desirable on the resulting distribution of Fe^{2+}. There is a small excess of (Fe^{2+}+Mg^{2+}) with respect to the $M(1)$ and $M(3)$ sites. Based on cationic size criteria it would be expected that Mg^{2+} would preferentially occupy the $M(2)$ site at the expense of Fe^{2+}; however, in this amphibole, as can be seen in table II, all the excess Fe^{2+} is found in the $M(2)$ site with the excess Mg^{2+} occupying the $M(4)$ site. The presence of Fe^{2+} in $M(2)$ is consistent with Mössbauer site-populations in alkali amphiboles (Bancroft *et al.*, 1969) but the lack of Fe^{2+} in $M(4)$ is surprising. In view of this result, further work on the Mössbauer spectrum of this amphibole is in progress.

The A-site. In the final stages of the refinement, with all isotropic temperature factors and an *R*-value of 6·0 %, the temperature factor of the *A*-site was 5·4 Å^2 which by comparison with other structures containing Na and K (Clarke *et al.*, 1969; Bailey, 1969; Brown *et al.*, 1969) is an unrealistically large value. The occupancy of the site

TABLE IV. *Selected interatomic angles*

T(1) Tetrahedron		*T(2) Tetrahedron*	
$O(1)$–$T(1)$–$O(5)$	109·8(2)°	$O(2)$–$T(2)$–$O(4)$	115·9(2)°
$O(1)$–$T(1)$–$O(6)$	109·9(3)	$O(2)$–$T(2)$–$O(5)$	109·6(2)
$O(1)$–$T(1)$–$O(7)$	111·2(3)	$O(2)$–$T(2)$–$O(6)$	108·6(2)
$O(5)$–$T(1)$–$O(6)$	105·2(2)	$O(4)$–$T(2)$–$O(5)$	109·1(2)
$O(5)$–$T(1)$–$O(7)$	109·6(3)	$O(4)$–$T(2)$–$O(6)$	103·0(2)
$O(6)$–$T(1)$–$O(7)$	111·0(3)	$O(5)$–$T(2)$–$O(6)$	110·5(2)
Mean O–$T(1)$–O	109·4	Mean O–$T(2)$–O	109·5
M(1) Octahedron		*M(3) Octahedron*	
$O(1^u)$–$M(1)$–$O(2^d)$	80·3(1)	$O(1^u)$–$M(3)$–$O(1^d)$	75·3(2)
$O(1^u)$–$M(1)$–$O(2^u)$	97·2(1)	$O(1^u)$–$M(3)$–$O(1^u)$	104·7(2)
$O(1^u)$–$M(1)$–$O(3^d)$	85·3(2)	$O(1^u)$–$M(3)$–$O(3^d)$	83·9(1)
$O(1^u)$–$M(1)$–$O(3^u)$	97·4(2)	$O(1^u)$–$M(3)$–$O(3^u)$	96·2(1)
$O(2)$–$M(1)$–$O(2)$	87·7(2)	Mean O–$M(3)$–O	90·0
$O(2)$–$M(1)$–$O(3)$	96·2(2)		
$O(3)$–$M(1)$–$O(3)$	79·9(3)	*M(4) Polyhedron*	
Mean O–$M(1)$–O	90·0	$O(2)$–$M(4)$–$O(2)$	77·2(2)
		$O(2^u)$–$M(4)$–$O(4^d)$	73·8(1)
M(2) Octahedron		$O(2^u)$–$M(4)$–$O(4^u)$	83·9(1)
$O(1)$–$M(2)$–$O(1)$	81·0(3)	$O(2^u)$–$M(4)$–$O(5^u)$	84·8(2)
$O(1^u)$–$M(2)$–$O(2^d)$	85·1(1)	$O(4^u)$–$M(4)$–$O(5^d)$	83·5(1)
$O(1^u)$–$M(2)$–$O(2^u)$	93·7(1)	$O(4^u)$–$M(4)$–$O(6^u)$	63·7(1)
$O(1)$–$M(2)$–$O(4)$	91·4(2)	$O(5^u)$–$M(4)$–$O(6^d)$	71·8(2)
$O(2^u)$–$M(2)$–$O(4^d)$	92·0(1)	$O(5^u)$–$M(4)$–$O(6^u)$	62·5(1)
$O(2^u)$–$M(2)$–$O(4^u)$	89·1(1)	$O(6)$–$M(4)$–$O(6)$	89·5(2)
$O(4)$–$M(2)$–$O(4)$	96·8(3)	Mean O–$M(4)$	75·9
Mean O–$M(2)$–O	90·0		
		Tetrahedral chain	
*A Polyhedron**		$T(1)$–$O(5)$–$T(2)$	133·7(2)
$O(7)$–$O(7)$–$O(7)$	65·8(1)	$T(1)$–$O(6)$–$T(2)$	140·7(2)
$\Delta = 0{\cdot}269$		$T(1)$–$O(7)$–$T(1)$	141·9(4)
$O(3')$–$O(3)$–H	100(9)	$O(5)$–$O(6)$–$O(5)$	164·4(2)
		$O(5)$–$O(7)$–$O(6)$	163·1(3)

* $\Delta = 90° - \measuredangle [O(7)\text{–}O(7)\text{–}O(7)]/90°$.

was allowed to vary but there was little change, and no improvement in the temperature factor.

Fig. 2 shows a series of Fourier sections parallel to (100) and at regular intervals down the $a \sin \beta$ direction. The sections are in the vicinity of the *A*-site. Electron-density highs can be seen on the 2-fold axis and also in the mirror plane. This was interpreted as two non-equivalent cation positions, one along the 2-fold axis and one

confined to the mirror plane. Consequently the *A*-site was positionally disordered to the two positions (0, *y*, 0) and (x, $\frac{1}{2}$, z), and the structure was refined. Starting positional parameters and occupancies for the refinement of these *A*-site positions were taken from Fourier maps and the isotropic temperature factors were set at 1·5° Å^2, this being a reasonable value for Na^+ and K^+ in silicates. Refinement of the positional

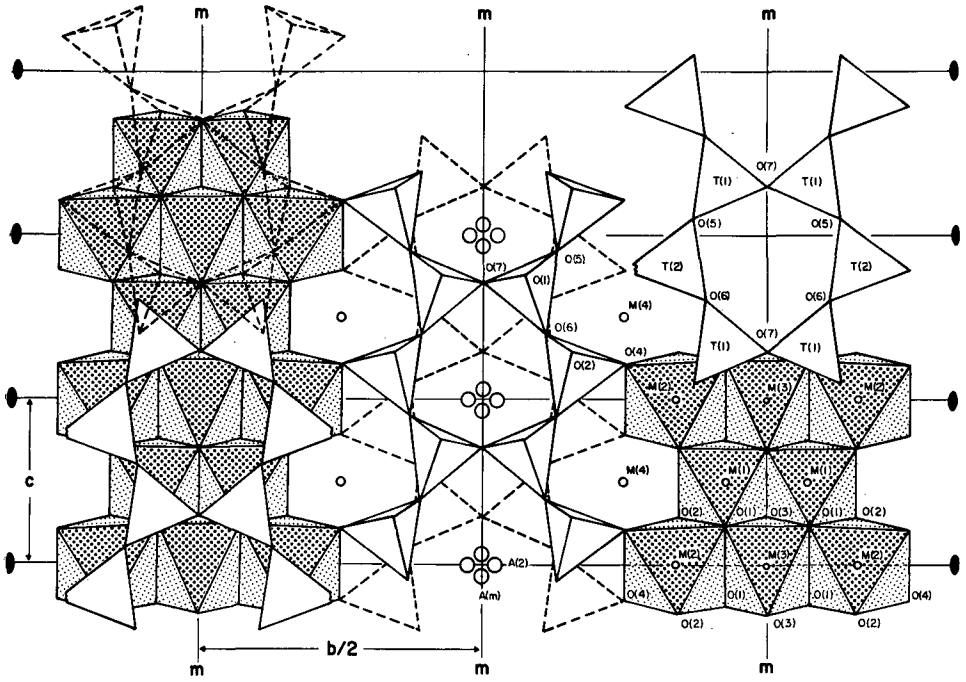

FIG. 1. A schematic scaled projection of the ferrotschermakite structure down the normal to (100). Note the positional disorder of the *A*-site.

parameters, occupancies, and temperature factors resulted in an *R*-factor reduction from 6·0 % to 5·9 % and a weighted R_w-factor reduction from 6·3 % to 6·1 % where $R_w^2 = \Sigma\, w(|F_0|-F_c|)^2/\Sigma\, F_0^2$ and $w = 1$. This improvement is significant at the 0·005 level (Hamilton, 1965).

In the final stages of refinement, 'the disordered *A*-site' chemistry was constrained to the 'bulk *A*-site' chemistry. Because the sites are only partially occupied, populations of Na^+ and K^+ cannot be used as separate variables. Consequently, the species Na^+ and K^+ were combined, and the vacancies were treated as a separate species with zero scattering power. Thus the populations of the two split *A*-sites are known purely as numbers of electrons and cannot be separated into Na^+ and K^+ populations.

In previous refinements of hornblende and potassium richterite (Papike *et al.*, 1969) positional disorder at the *A*-site was present. Only the position disordered in the mirror plane was refined, although mention is made of electron density being present on the

2-fold axis. This is in accord with the present findings where the positions in the mirror plane show a site-preference over the one on the 2-fold axis. Papike *et al.* suggested that the extra density at the position on the 2-fold axis may be due to Na^+ and K^+ occupying slightly different positions. This is not found in this case as the electron densities at the two positions do not agree with the amounts of Na^+ and K^+

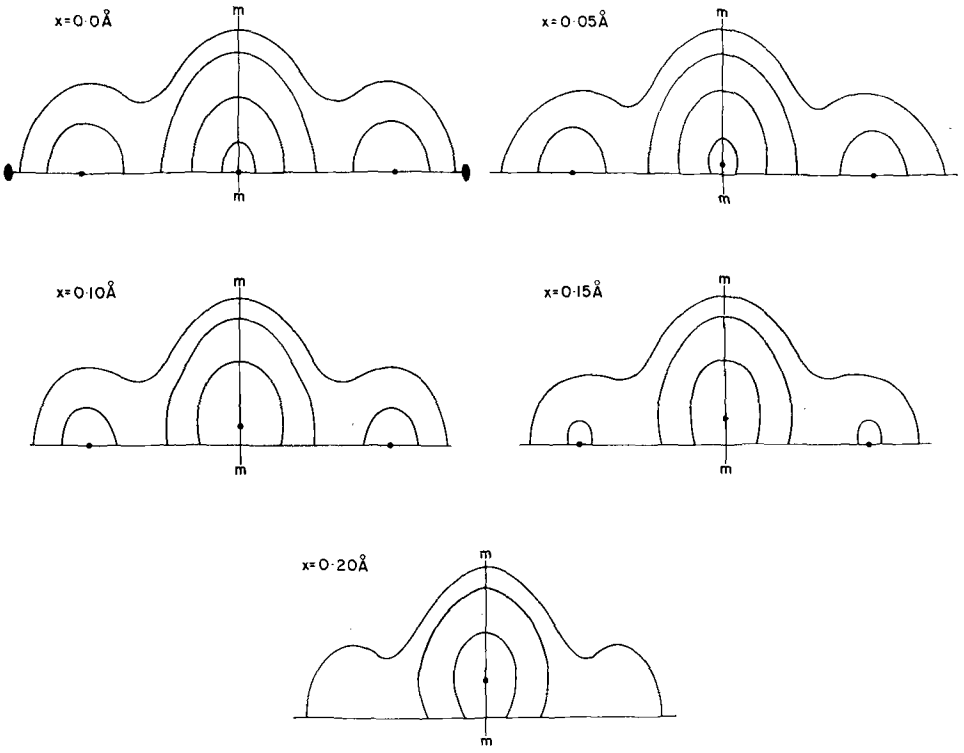

FIG. 2. Diagram shows a series of Fourier sections taken in the vicinity of the *A*-site perpendicular to the normal to (100). X distance along the *a* direction, section X = 0·0 Å is through the *A*-site; m mirror plane; ⬮ diad; ● location of maxima in electron density.

in the *A*-sites given by the chemical analysis. This would suggest that the type of species present is not the major factor in controlling the direction of disordering. Gibbs and Prewitt (1968) suggested that the anion occupancy of the *O*(3) position controls the direction of disorder. This effect is precluded in this case as the amphibole under investigation contains insignificant amounts of F^-.

As suggested by Papike *et al.* (1969), the main factor in determining the exact position of the *A*-site cation is apparently the distribution of tetrahedral Al and the resulting charge-balance requirements. However, another possibly important factor could be the multivalent substitution of cations in the octahedral sites and the resultant charge-balance and cation–cation repulsive forces. Because of the uncertainty

of the distribution of tetrahedral Al and the possible interaction of a number of factors controlling the *A*-site disorder, more experimental work is in progress in order to resolve this problem.

In view of the double nature of the *A*-site disorder, the following site nomenclature is proposed: *A* or *A*(2/*m*) 0, ½, 0; *A*(*m*) *x*, ½, *z*; *A*(2) 0, *y*, 0.

TABLE V. *Occupancies of T*(1) *and T*(2)

1	*T*(1) = (0·38 Al+0·62 Si)	*T*(2) = (0·12 Al+0·88 Si)
2	(0·45 Al+0·55 Si)	(0·05 Al+0·95 Si)
3	(0·31 Al+0·69 Si)	(0·19 Al+0·81 Si)
4	(0·46(3) Al+0·54(3) Si)	(0·04(3) Al+0·96(3) Si)

1. Average *T–O* distances in a number of amphibole structures are used to establish a Smith–Bailey plot. Mean *T–O* distance for complete Si occupancy is 1·623 Å (Papike *et al.*, 1969) and mean *T–O* distance for 25% Al occupancy is 1·655 Å in the Kakanui hornblende. This gives the equation $(T\text{–}O) - 1{\cdot}623 = 0{\cdot}128 \times$ (fractional Al occupancy).
2. The amount of Al determined by chemical analysis as assigned by comparison of the mean *T–O* distances in the ferrotschermakite to those of tremolite.
3. Mean *T–O* non-bridging distances are used as in 2.
4. Occupancies derived by chemically-constrained site-refinement (Finger, 1969*a*).

Tetrahedral sites. The *T*(1) site is larger and more regular than the *T*(2) site, and is coordinated by three bridging and one non-bridging oxygen atoms while the smaller *T*(2) site is coordinated by two bridging and two non-bridging oxygen atoms. The distribution of tetrahedral aluminium between *T*(1) and *T*(2) was estimated after the methods of Papike *et al.* (1969)[1] and also determined by chemically-constrained site-refinement (Finger, 1969*a*). The occupancies derived from each method are presented in table V. The results of the site-refinement would indicate that the second method of estimation by Papike *et al.* (1969) gives the most consistent results.

The anisotropic thermal model. The temperature factor form used was

$$\exp\Big[-\sum_{i=1}^{3}\sum_{j=1}^{3} h_i\, h_j\, \beta_{ij}\Big]$$

and the anisotropic temperature factor coefficients are given in table VI. The magnitudes and orientations of the principal axes of the thermal ellipsoids were calculated using the programme ERRORS (Finger, personal communication) and are presented in table VII, and visually as a stereoscopic drawing in fig. 3.

Since the occupancies of all the cation sites are disordered, the magnitudes of all temperature factors will be increased by slight positional disorder resulting from differential relaxations around the cation sites according to which species is present. However, the directions of vibration should not be greatly affected. Both the *T*(1) and *T*(2) ellipsoids are fairly isotropic with the maximum vibration direction nearly perpendicular to the maximum tetrahedral edge lengths. The maximum vibration

[1] See footnote to Table V.

TABLE VI. *Temperature factor coefficients for ferrotschermakite*

Atom	B_{ISO} or B_{11}	B_{22}	B_{33}	B_{12}	B_{13}	B_{23}
T(1)	0·00189(12)	0·00036(3)	0·00544(41)	−0·00013(5)	0·00073(18)	0·00001(9)
T(2)	0·00203(12)	0·00034(3)	0·00503(38)	0·00001(4)	0·00097(17)	0·00007(9)
M(1)	0·00278(12)	0·00038(3)	0·00523(38)	0	0·00181(17)	0
M(2)	0·00201(15)	0·00029(3)	0·00495(49)	0	0·00064(21)	0
M(3)	0·00252(15)	0·00021(3)	0·00548(50)	0	0·00059(22)	0
M(4)	0·00316(14)	0·00051(3)	0·00802(44)	0	0·00233(19)	0
O(1)	0·00287(33)	0·00087(9)	0·00812(113)	−0·00014(15)	0·00126(49)	−0·00015(27)
O(2)	0·00222(31)	0·00060(8)	0·00733(108)	−0·00002(13)	0·00077(45)	−0·00009(24)
O(3)	0·00419(54)	0·00059(12)	0·00781(69)	0	0·00285(77)	0
O(4)	0·00357(33)	0·00033(8)	0·01034(120)	−0·00029(13)	0·00297(51)	0·00016(24)
O(5)	0·00261(32)	0·00085(9)	0·00811(110)	−0·00009(14)	0·00071(47)	0·00084(26)
O(6)	0·00306(34)	0·00068(8)	0·00996(115)	−0·00013(14)	0·00153(51)	−0·00099(26)
O(7)	0·00414(56)	0·00071(13)	0·01722(204)	0	0·00304(87)	0
A(*m*)	1·74(7)					
A(2)	1·30(5)					
H	0·50					

TABLE VII. *Ellipsoids of vibration and equivalent isotropic temperature factor*

Atom	R.M.S. Displacement	Angle to *a*-axis	Angle to *b*-axis	Angle to *c*-axis	Atom	R.M.S. Displacement	Angle to *a*-axis	Angle to *b*-axis	Angle to *c*-axis
T(1)	0·074(3) Å²	70(7)°	20(7)°	96(13)°	*O*(1)	0·104(7)	92(36)	80(24)	16(39)
	0·085(3)	93(13)	88(13)	162(13)		0·112(7)	152(26)	118(27)	74(40)
	0·096(3)	20(7)	110(7)	107(13)		0·123(6)	62(26)	150(24)	87(17)
T(2)	0·075(3)	93(7)	163(13)	73(13)	*O*(2)	0·097(7)	67(90)	113(140)	45(37)
	0·086(3)	75(12)	107(13)	163(13)		0·099(7)	121(80)	147(112)	91(110)
	0·097(3)	15(12)	88(7)	90(12)		0·105(7)	140(45)	68(46)	45(37)
M(1)	0·076(3)	115(3)	90	10(3)	*O*(3)	0·091(12)	116(9)	90	11(9)
	0·079(3)	90	0	90		0·099(10)	90	0	90
	0·114(2)	25(3)	90	80(3)		0·140(9)	26(9)	90	79(9)
M(2)	0·070(4)	90	0	90	*O*(4)	0·065(10)	71(7)	23(9)	107(8)
	0·082(4)	93(11)	90	162(11)		0·106(7)	54(10)	112(9)	149(10)
	0·097(4)	3(11)	90	108(11)		0·135(6)	42(9)	97(6)	64(10)
M(3)	0·059(5)	90	0	90	*O*(5)	0·091(8)	92(18)	125(9)	36(7)
	0·086(4)	96(6)	90	159(6)		0·108(7)	157(12)	108(15)	90(17)
	0·110(3)	6(6)	90	111(6)		0·133(6)	113(12)	40(8)	54(7)
M(4)	0·092(3)	90	0	90	*O*(6)	0·086(8)	92(11)	39(7)	52(7)
	0·093(3)	55(4)	90	160(4)		0·117(7)	176(19)	94(16)	74(18)
	0·123(3)	35(4)	90	70(4)		0·131(6)	86(22)	129(7)	43(11)
					O(7)	0·109(10)	90	0	90
						0·131(10)	165(19)	90	60(19)
						0·153(9)	75(19)	90	30(19)

directions of the bridging oxygens $O(5)$, $O(6)$, and $O(7)$ are perpendicular to the bridging bonds, indicating that the bending moments are much less than the corresponding stretching moments.

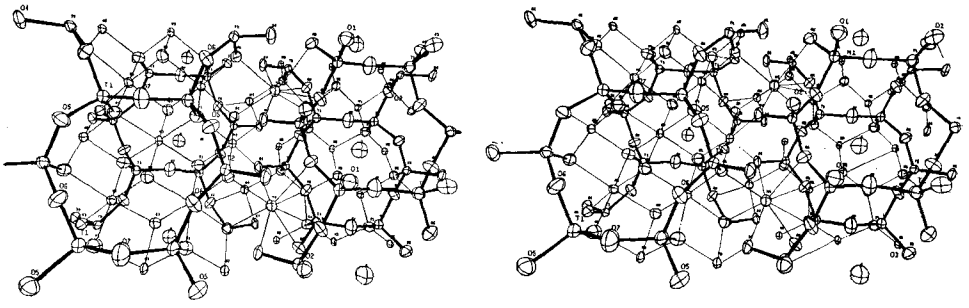

FIG. 3. A stereoscopic drawing of the ferrotschermakite structure viewed approximately down the direction normal to (100) showing probability ellipsoids of thermal vibration. The solid lines represent bond directions that are associated with the chains of tetrahedra. The fine lines show the direction of other bonds in the crystal.

The octahedral cations have their maximum vibration direction perpendicular to the largest octahedral face in each site, corresponding to the direction of least bond stretching (Megaw, 1968). The $M(4)$ cation has its maximum vibration direction approximately along the long diagonal of the polyhedron. Of the octahedrally coordinating oxygens, only $O(4)$ shows any degree of anisotropy; the $O(4)$ ellipsoid is an ellipsoid of revolution with the long axis sub-parallel to the long axis of the $M(4)$ ellipsoid. This would suggest that the vibrations of $M(4)$ and $O(4)$ are coupled.

Acknowledgements. One of the authors (H. D. Grundy) is grateful to the National Research Council of Canada and the Geological Survey of Canada for research grants awarded to assist this work. The authors would like to thank the International Nickel Company for supplying the specimens and also are indebted to Dr. C. Calvo and to Dr. B. J. Burley for critical review and discussion of the manuscript.

REFERENCES

ALEXANDER (L. E.) and SMITH (G. E.), 1964. *Acta Cryst.* **17**, 1195–1201.
BAILEY (S. W.), 1969. *Amer. Min.* **54**, 1540–5.
BANCROFT (G. M.) and BURNS (R. G.), 1969. *Min. Soc. Amer. Spec. Pap.* **2**, 137–48.
BROWN (G. E.) and GIBBS (G. V.), 1969. *Amer. Min.* **54**, 101–16.
CLARK (J. R.), APPLEMAN (D. E.), and PAPIKE (J. J.), 1969. *Min. Soc. Amer. Spec. Pap.* **2**, 31–50.
CROMER (D. T.) and MANN (J. B.), 1968. *Acta Cryst.* **A24**, 321–4.
DOLLASE (W. A.), 1969. *Zeits. Krist.* **132**, 27–44.
DOYLE (P. A.) and TURNER (P. S.), 1968. *Acta Cryst.* **A24**, 390–7.
FINGER (L. W.), 1969*a*. *Carnegie Inst. Wash. Year Book*, **67**, 216–17.
—— 1969*b*. *Min. Soc. Amer. Spec. Pap.* **2**, 95–100.
GIBBS (G. V.) and PREWITT (C. T.), 1966. *Abstr. Int. Min. Ass. Pap. Proc. 5th Gen. Meet.* Mineralogical Society, London, 1968, 334–5.
HAMILTON (W. C.), 1965. *Acta Cryst.* **18**, 502–10.
MEGAW (H. D.), 1968. Ibid. **B24**, 149–53.

PAPIKE (J. J.), ROSS (M.), and CLARK (J. R.), 1969. *Min. Soc. Amer. Spec. Pap.* **2**, 117–36.
ROBINSON (K.), GIBBS (G. V.), and RIBBE (P. H.), 1969. Abstr. *Amer. Min.* **55**, 307.
SHANNON (R. D.) and PREWITT (C. T.), 1969. *Acta Cryst.* **B25**, 925–46.
SMITH (J. V.) and BAILEY (S. W.), 1963. Ibid. **16**, 80–110.
TOKONAMI (M.), 1965. Ibid. **A19**, 486.

[*Manuscript received 6 March 1972*]

Note added in proof: Full details of the 1747 reflections have been deposited as NAPS document 01807, and may be obtained from Microfiche Publications, 305 East 46 Street, New York, N.Y. 10017, U.S.A.